

polarisé, rectilignement dans l'onde homogène et elliptiquement dans l'onde inhomogène. Cette ellipticité est liée à l'incidence, le rapport des composantes pouvant varier entre 0 et 0,5 (pour  $i_c$  variant de  $i_c$  à 90° par exemple).

La mesure des facteurs de dépolarisation est très perturbée par l'ouverture des faisceaux dans le microscope; dans le cas des expériences avec le spectromètre seul, on peut, avec quelques approximations, tirer des renseignements sur les orientations des champs.

### Conclusion

Plutôt que de résumer ici les méthodes, il convient sans doute de résumer leurs possibilités.

L'utilisation des ondes homogènes permet l'étude des problèmes de structure et d'interaction dans des films d'épaisseur supérieure à 140 nm.

L'utilisation des ondes évanescentes permet d'atteindre les monocouches et, dans ces conditions, d'étudier les ondes de surface, les interactions avec une solution ou la structure d'une monocouche au voisinage d'une interface. On peut étudier ainsi des problèmes aussi différents que :

- la catalyse,
- l'adsorption,
- les ondes de surface,
- les phénomènes d'électrolyse,
- les problèmes de perméabilité des membranes biologiques ou d'hémocompatibilité.

Le Raman de résonance facilite la prise des spectres.

Il est certain que, pour l'instant, les mesures de facteurs de dépolarisation sont, ou approximativement exploitées, ou difficilement exploitables.

La microsonde Raman seule n'est pas directement utilisable pour l'étude des films minces, sauf dans le cas de la résonance; un dispositif auxiliaire doit être envisagé.

### Bibliographie

- (1) Harrick, Internal reflection spectroscopy, Interscience N-Y (1967)
- (2) A. Hjortsberg, W. P. Chen et E. Burstein, *Optics Comm.*, 1978, **25**, 1, 65.
- (3) I. Pockrand, J. D. Swalen, R. Santo, A. Brillante et M. R. Philpot, *J. Chem. Phys.*, 1978, **69** (9), 4001.
- (4) T. Takenaka et T. Nakanaga, *J. of Phys. Chem.*, 1976, **80**, 475. T. Nakanaga et T. Takenaka, *J. of Phys. Chem.*, 1977, **81**, 7, 645. T. Takenaka et H. Fukuzaki, *J. of Raman Spect.*, 1979, **8**, 3, 151. T. Takenaka, *Advances in colloid and Int. Science*, 1979, **11**, 291.
- (5) Wessler, Rödel et P. Friese, *Experimentelle Technik der Phys.* XXI, 1973, **4**, 343.
- (6) J. Cipriani, H. Hasmonay, Y. Levy, S. Racine, M. Dupeyrat, R. Dupeyrat and C. Imbert, *Japan J. Appl. Phys.*, 1975, **14**, suppl. 14-1, 93 (Communication au congrès de Tokyo en 1974).
- (7) Y. Levy, C. Imbert, J. Cipriani, S. Racine and R. Dupeyrat, *Optics Communications*, 1974, **11**, n° 1, 66.
- (8) J. Cipriani, S. Racine, R. Dupeyrat, H. Hasmonay, M. Dupeyrat, Y. Levy and C. Imbert, *Optics Com.*, 1974, **11**, n° 1, 70.
- (9) M. Masson, H. Royer, R. Dupeyrat et J. P. Laude, *Optics Com.*, 1977, **20**, n° 3, 162.
- (10) M. Menetrier, R. Dupeyrat, Y. Levy et C. Imbert, *Optics Com.*, 1977, **21**, n° 1, 162.
- (11) M. Delhayé, M. Dupeyrat, R. Dupeyrat et Y. Levy, *Journal of Raman Spectroscopy* (1979).
- (12) A. Aurengo, M. Masson, R. Dupeyrat, Y. Levy, H. Hasmonay et J. Barbillat, *Bioch. Biophys. Research Comm.*, 1979, **89**, 2, 559.
- (13) Dhamelin court, Thèse à Lille (1979)

## Use of computerized image processing systems for enhanced image quality with the Mole

by F. Adar \*, P. Dhamelin court \*\*, R. Grayzel \* and D. London \*

(\* ISA, Inc, 173 Essex Avenue, Metuchen 08840, N. J., U.S.A. et \*\* CNRS, Université des Sciences et Techniques de Lille, U.E.R. de Chimie, Laboratoire de spectrochimie infrarouge et Raman, 59650 Villeneuve d'Ascq, France)

### Utilisation de systèmes de traitements pour améliorer la qualité des images Raman

En vue d'améliorer la qualité des images Raman obtenues avec la Mole, plusieurs systèmes de traitements d'image digitaux ont été testés dans notre Laboratoire d'applications Mole, à Metuchen : leur méthode de moyennage permet de supprimer le bruit engendré par le tube intensificateur d'images et le tube vidicon SIT. De plus, l'utilisation de leur mémoire digitale permet de comparer deux images, l'une obtenue dans une raie Raman, et l'autre en dehors de cette même raie. Cela est très important pour soustraire le fond de fluorescence des images observées.

Des images de bonne qualité ont été obtenues avec des sphères de  $ThO_2$  et de polystyrène placées sur un papier donnant un fond de fluorescence de 3 à 10 fois plus intense que les signaux Raman. De plus, nous avons constaté que la qualité de l'image obtenue n'était limitée que par la capacité du système à différencier deux signaux intenses et que statistiquement cette qualité s'améliorait avec le temps d'intégration du signal.

In addition to the Mole's capability to function as a molecular microprobe, we all know that it has a unique optical system providing the capability to produce Raman images of heterogeneous samples. While this capability for mapping a particular species in a heterogeneous sample has enormous potential to the scientific and technological community, success in many applications has been hampered by the inherent limitations of image detectors and the presence of fluorescence background from the samples themselves superimposed on relatively weaker Raman signals.

Comparison of the performance of the best photomultiplier detector

with the best imaging detector indicates that in the first instance the noise of the signal is completely determined by the theoretical noise generated by randomly occurring events (Raman photon emission) whereas there is substantial electronic and thermal noise in image detectors that will not be eliminated in the near future. It is important to realize that Raman signals themselves pose problems for even the best detectors. The signals from many materials tend to be weak. This requires operating the detectors at maximum gain, which will increase the noise of the detector and cause a non-linear response in regions of the field of view where the images are stronger. Another problem inherent to the technique is the frequent presence of

fluorescent backgrounds which can be comparable to or stronger than the Raman signals of interest.

In an attempt to improve the Raman image quality on the Mole we have tested image processors that digitize the images on the vidicon, store them in an array, and provide the ability to perform simple arithmetic operations on the images.

In order to test the capability of the Mole with an image processor to produce recognizable Raman images of samples, we examined spheres of  $\text{ThO}_2$  and polystyrene on fluorescing paper. These samples were chosen because the spheres are visually easy to recognize and because the signals are known to scale with size. We also know that the signal from a polystyrene sphere is approximately an order of magnitude weaker than that from a similar size sphere of  $\text{ThO}_2$  taken under identical conditions. Thus the experiments dealt with both a relatively easy and a more realistic sample.

Our data that follows will be presented in a sequence that will demonstrate how the image processor deals with each source of noise.

The following images were achieved with a SEC camera. Because the camera itself does not generate noise, it is possible to integrate on the camera for substantial periods of time before reading out the data.

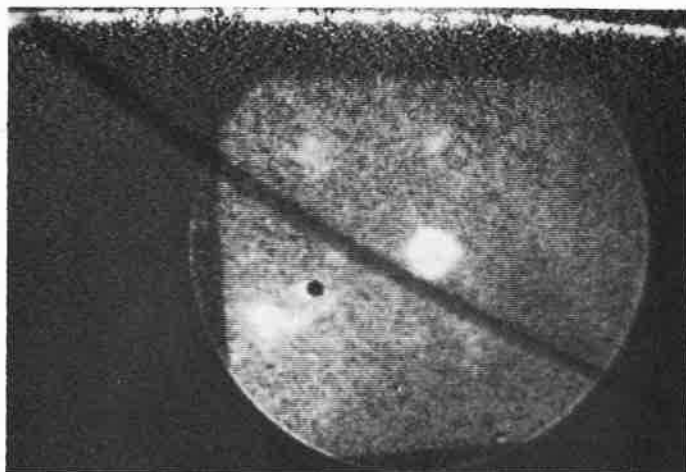


Figure 3. Raman image of sample as in figure 2 after subtracting fluorescent background.

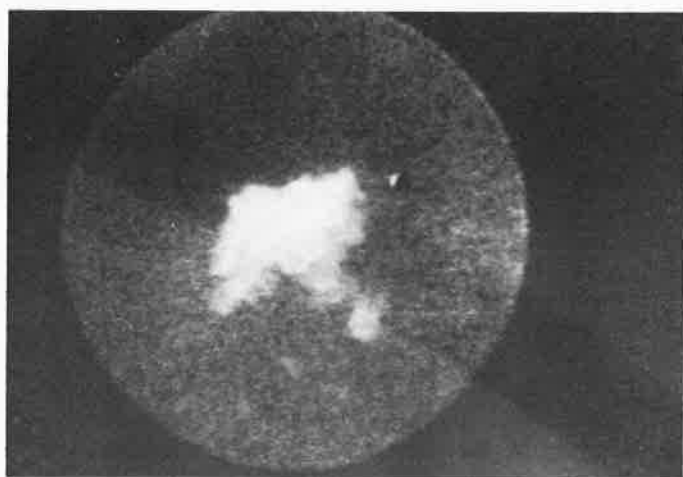


Figure 1. Raman image at  $467\text{ cm}^{-1}$  of a cluster of  $\text{ThO}_2$  spheres on a sapphire substrate.

The images were integrated for 5 seconds on a SEC vidicon. After A/D conversion, 60 such images were accumulated in the memory. 450 mW of laser radiation at 514,5 nm entered the Mole. The 32x objective was installed in the Ultropak.

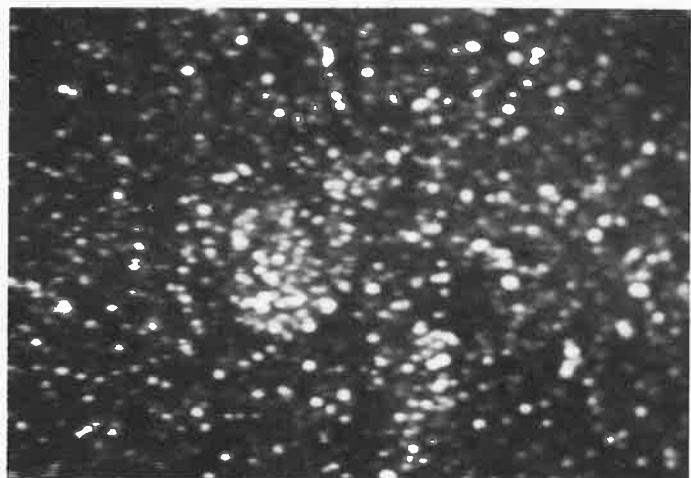


Figure 4. Real time Raman image of  $\text{ThO}_2$  spheres on glass slide as detected by a SIT vidicon. Illumination conditions as above.



Figure 2. Raman image of  $\text{ThO}_2$  spheres on fluorescent paper as detected by SEC vidicon.

This image represents 60 3 second integrations. Other conditions were as above.

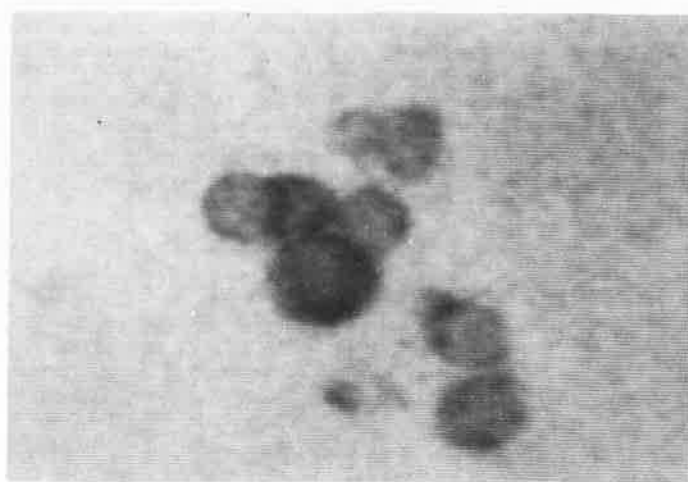
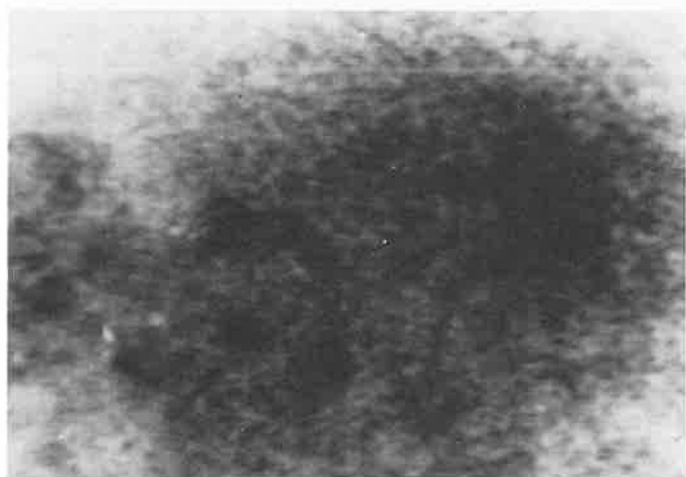
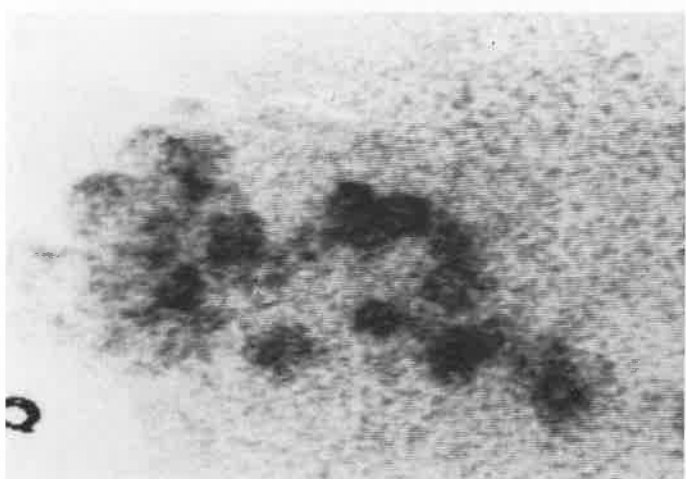


Figure 5. Moving average of same sample as shown in figure 4. This picture represents a 16 second time averaged image.



**Figure 6.** Moving average of  $\text{ThO}_2$  spheres on fluorescent paper as detected by SIT vidicon.



**Figure 7 a.** SIT Raman image of  $\text{ThO}_2$  spheres on fluorescing paper integrated for 32 seconds and then background subtracted.

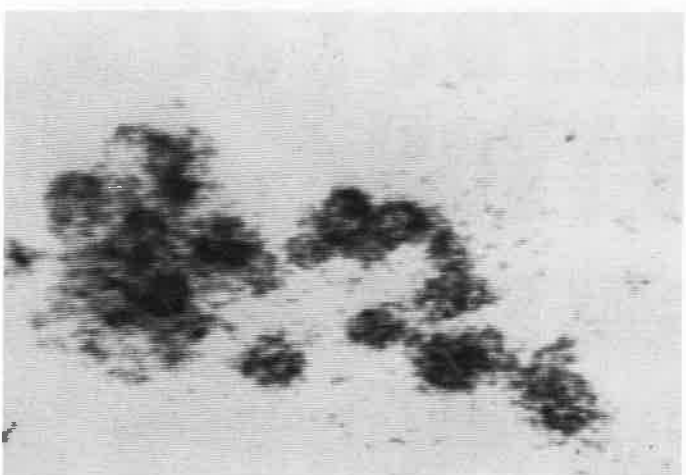


**Figure 7 b.** Same as a, but with additional background subtraction to compensate for decaying fluorescence.

The first slide shows the image produced from a cluster of  $\text{ThO}_2$  spheres dispersed on a sapphire substrate. This image was generated by 450 mW of 514,5 nm radiation entering the Mole and by summing 60 5 - second integrations. It was noted that during sep-uP the A/D converter was set to quantize the grey level so that the noise in the

image was greater than the smallest step in the grey. Under these conditions a long integration averages the noise. The slide shows clearly defined spheres; in addition, the circular field surrounding the spheres is somewhat darkened by the background produced by the image intensifier.

The next slide shows an integrated image of  $\text{ThO}_2$  spheres dispersed on fluorescing paper. This image was taken with 60 3 - sec. integrations before background subtraction. The intensity of the fluorescence relative to the Raman can be judged by examination of the contrast. The next slide shows an image of the same sample after subtracting the fluorescence. This was achieved by rotating the gratings by about  $50 \text{ cm}^{-1}$ ; at such a position, the fluorescence is broad and is relatively unchanged, whereas the Raman signal is absent.

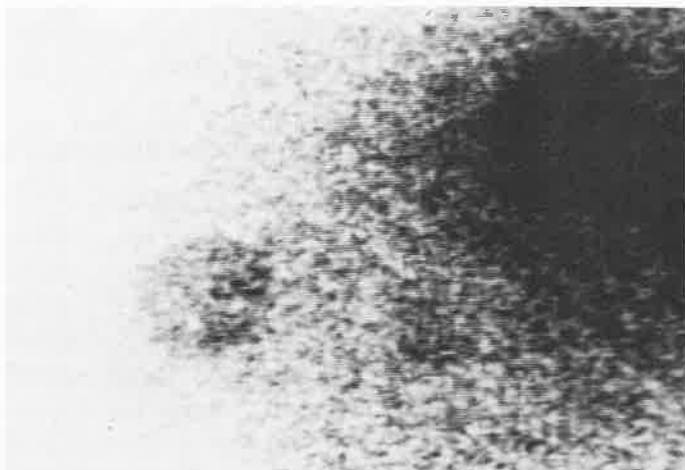


**Figure 8.** Raman image of polystyrene spheres at  $1006 \text{ cm}^{-1}$ , as detected by SIT vidicon, integrated for 10 minutes and background subtracted.

We also made tests with a SIT camera in place of the SEC. It is well known that a SIT camera has a large amount of noise generated by the silicon target. This noise is often comparable in intensity to Raman signals. Thus it is necessary with such a system to suppress the camera background before any work can be done on even the simplest of samples. This is achieved by taking a moving average of the signal, (*ie*, for averaging  $N$  frames the signal from each frame is divided by  $N$  and added to  $1 - \frac{1}{N}$  times the memory. The A/D

converter is set up for «photon counting»), a photon event is counted and other scintillations are suppressed as much as possible. The next slide shows a real time image of  $\text{ThO}_2$  spheres on a glass slide; the spheres are barely recognizable. The following slide shows a moving average image of the same sample. The real time image represents 16 msec of data, whereas the moving average represents 16 sec time averaged.

The next slide shows a moving average (16 sec) image of the  $\text{ThO}_2$  spheres mounted on fluorescing paper. Because of the fluorescence the contrast is poor. The next slide shows an image of the same sample from which fluorescence background was subtracted from the signal integrated for 32 sec. Again the improvement in contrast after background subtraction is striking.

As a final example we imaged polystyrene spheres on the same fluorescent paper. In this case it was possible to produce a recognizable image only after 10 minutes integration. While the spheres are visible in the slide, the image quality is admittedly poorer than the previous example. The mottled nature of this image is determined by the noise remaining after background subtraction of the Raman image. Since this noise can be comparable to the Raman signal, the statistics of the subtracted image can be improved by increasing the integration times. This slide indicates, however, that the Mole is capable of producing Raman images of samples in the presence of fluorescence backgrounds.